Wavelet intermittent blowout detection in thermoacoustic instability of trapped vortex combustor

To cite this article: Tiziano Pagliaroli and Guido Troiaini 2020 *J. Phys.: Conf. Ser.* **1589** 012005

Journal of Physics: Conference Series **1589** (2020) 012005 doi:10.1088/1742-6596/1589/1/012005

Wavelet intermittent blowout detection in thermoacoustic instability of trapped vortex combustor

Tiziano Pagliaroli[1], Guido Troiaini[2]

[1] Università Niccolò Cusano, Via Don Carlo Gnocchi 3, 00166 Rome, Italy
[2] ENEA C.R. Casaccia, Via Anguillarese 301, 00123 Roma, Italia

E-mail: `tiziano.pagliaroli@unicusano.it`

Abstract. This paper is aimed to the study of spontaneous radiant energy emitted by trapped vortex flame, focusing on the intermittent occurrence of flame blowout during thermoacoustic oscillation. We tackle this issue by a wavelet–based auto–conditioning technique, able to detect intermittent structures in the radiant energy signal, which we identify as a trace of extinction–reignition events. Intermittent events are found to be in phase with the tonal component of the radiant energy signal, although they occur randomly in time. Despite the wavelet auto–conditioning technique is a well established method in fluid dynamics and aeroacoustics, our work represents the first application in combustion field.
Additional information about blow–out are inferred by analysing the average signature computed from the radiant power time series: re–ignition velocity appears higher than extinction velocity. This result confirms the effectiveness of the radiant power for combustion diagnostics.

1. Introduction

Gas turbines, rocket engines, furnaces and boilers are often affected by the first transition from stable combustion regime to thermoacoustic instability, which arises in high–amplitude self–excited pressure oscillations. This unstable regime may induce structural vibrations shortening the system lifespan or leading to reduction in combustion efficiency. In some cases, a second transition process may follow on, leading the flame from instability to blow–out [1].
Over the last years, most experimental studies have focused on the first transition process, addressing their efforts to the analysis of pressure signals for the identification of the so–called 'intermittency', regarded as precursors of the transition from stable to unstable regime. In addition, chaotic analysis has got a key role looking at pressure fluctuations in terms of attractor in pseudo–phase space and recurrence plots, which allow to identify the thermoacoustic instability precursors in large–amplitude oscillations evolving from stochastic to periodic [2, 3, 4, 5]. The present paper examines the transition from thermoacoustic instability to blowout, being it underrepresented in the literature. The mechanism underlying this second transition is investigated by analyzing the spontaneous radiant energy emitted by the flame.

Some relevant advantages can be identified with reference to radiant energy analysis: *i)* since this observable exhibits the same tonal components in Fourier domain as the pressure fluctuations during the thermoacoustic instability, it gives an overall description of thermoacoustic stability/instability behaviour [6]; *ii)* its spectrum reproduces the same characteristic decay as the inertial scaling of the kinetic energy for homogeneous, isotropic, non–reactive turbulent flows [7].

In the present paper, pressure and radiant energy are sampled in a Trapped Vortex Combustor (TVC), consisting in a cubical cavity and long neck. In recent years, this geometry has been already investigated from acoustic and aeroacoustic viewpoint, showing that TVC behaves as a Helmholtz resonator and the first acoustic mode dominates the wall pressure spectra also in the presence of a mean flow [8, 9]. Further, TVC has been investigated in reactive conditions, applying chaotic analysis to experimental database, as recently proposed by [10, 11].
We propose here a strategy for the analysis of the same TVC database, achieving, as main outcome, the identification of intermittent coherent structures in the radiative emission during the thermoacoustic instability, prior to flame blowout. Similar events, supposed to be the trace of flame extinction–reignition occurrences, were preliminary found by [12].

Being the presence of such events localized in time, extraction of the corresponding signatures is not feasible with standard techniques in the Fourier domain. Rather, wavelet–based techniques are more suitable options for this purpose. According to this claim, Wavelet–Based Autoconditioning Technique (WBAT), already used with success in aeroacoustics [13] and turbulence [14], is exploited to grab signatures within the broad band time history of radiant energy.

2. Wavelet-based method for intermittent events identification

2.1. Wavelet Transform

Wavelets are a relatively recent instrument developed in applied mathematics around thirty years ago [15] and have become a common and attractive tool for time series analysis. In particular, in the last two decades, wavelet transform (WT) has been used for a number of studies, e.g. capturing sea surface thermodynamic variable oscillations in ocean science [16], studying coherent structures in turbulent flows [15], signal denoising [17], studying intermittent phenomena in aeroacoustics and solid rocket motors [18, 19], and, very recently, investigating the acoustic behaviour of meta-surfaces for boundary layer transition control [20, 21]. In this section, a Wavelet–Based Auto–conditioning Technique (WBAT) is described as effective at capturing coherent structures embedded within time histories [13, 14] and providing average shape, occurrence and amplitude distributions of signal signatures.

WT permits to decompose a space/time history expanding the choice for a proper basis among a great variety of suitable functions, allowing to tailor the selected wavelet to each specific problem [22].

One of the main properties of wavelet basis functions is their localization in both time and frequency domains. As a result, wavelet series better fit wave forms usually found in nature and often converge faster than corresponding Fourier series. The starting point for continuous wavelet transform (CWT) consists in choosing a proper wavelet function $\psi(t)$, called the *mother* wavelet, which can be real or complex [23]. In particular, the present analysis is performed by selecting a real mother wavelet named Ricker (or mexican hat). Ricker mother function is proportional to the second derivative of the Gaussian function:

$$\psi(t) = \frac{2}{\sqrt{3}}\pi^{-\frac{1}{4}}(1-t^2)e^{-\frac{t^2}{2}} \tag{1}$$

where t is the dimensionless time [16, 15]. Grounded on the mother wavelet function ψ, a family of continuously translated and dilated wavelets (the orthogonal basis function) can be generated and normalized in energy norm:

$$\psi_{s,\tau}(t) = s^n \psi\left(\frac{t-\tau}{s}\right) \quad \forall\, s,\tau \in \mathbb{R}^+ \tag{2}$$

where s is the scaling parameter and τ the time shifting: an increase in s corresponds to dilation in time and contraction in frequency domain. The parameter n in eq. 2 is the normalization exponent such that

$$\int_{-\infty}^{\infty} |\psi_{s,\tau}|^2 dt = 1. \tag{3}$$

In the present analysis, L^2-normalization has been applied, thus $n = -1/2$. The continuous WT of the time signal $x(t)$ is therefore defined as:

$$w(s,\tau) = s^{-1/2} \int_{-\infty}^{+\infty} x(t)\psi^*_{s,\tau}(t)\,\mathrm{d}t \tag{4}$$

where $w(s,\tau)$ are the wavelet coefficients [18, 19, 24] and $(\cdot)^*$ denotes the complex conjugate of a function.

2.2. *Wavelet auto–conditioning*

An intermittent event can be seen as an high energetic and coherent structure well localized in time. In this framework, WBAT is supported by a dimensionless energy criterion called Local Intermittency Measure (LIM) defined as follows [15]:

$$LIM(s,\tau) = \frac{w^2(s,\tau)}{\langle w^2(s,\tau)\rangle_\tau} \ , \tag{5}$$

with $\langle\cdot\rangle_\tau$ the time averaging. This function enhances non-uniform distributions of energy in time, where the quantity $w^2(s,\tau)$ can be regarded as the energy content of the signal at a given scale s and instant τ. LIM(s,τ) provides a local measure in time–scale space of the energy deviations from the signal energy content averaged over time. The coherent event identification strategy here employed [25] is based on the idea that the passage of a signature with a specific scale s_i at the instant τ_i, results in a relative maximum in the LIM map at scale s_i and time τ_i. Thus, a thresholding procedure applied to LIM, fixing a proper threshold level T, allows to select a set of relative maxima satisfying the condition LIM$(\tau_i, s_i) > T$.

The i–th event is identified in the time domain in terms of reference time, $t = \tau_i$:

$$x|x\,(\tau_i,\xi) = x\,(\tau_i + \xi) \quad \forall \xi \in \Xi \tag{6}$$

being ξ a local time variable and $\div$ a function of the auto-correlation length, namely a time window wide enough to include the intermittent event (wider than a few times the temporal macro–scale). Hence the auto–conditional average of the raw signal reads:

$$\langle x|x\,(\tau_i,\xi)\rangle\ = \frac{1}{N}\sum_{i=1}^{N} x|x\,(\tau_i,\xi)\ , \tag{7}$$

where the symbol $\langle\cdot\rangle$ denotes the ensemble average. In order to highlight the weight of the signature in terms of statistical fluctuations, $\langle x|x\,(\tau_i,\xi)\rangle$ is normalized with respect to the signal standard deviation, $\langle x'^2\rangle^{1/2}$ (being x' the fluctuation of x).

Although Ricker wavelet is selected as mother wavelet because its shape is coherent with the events to be identified, the auto–conditioning technique here described is independent of the specific mother wavelet selected.

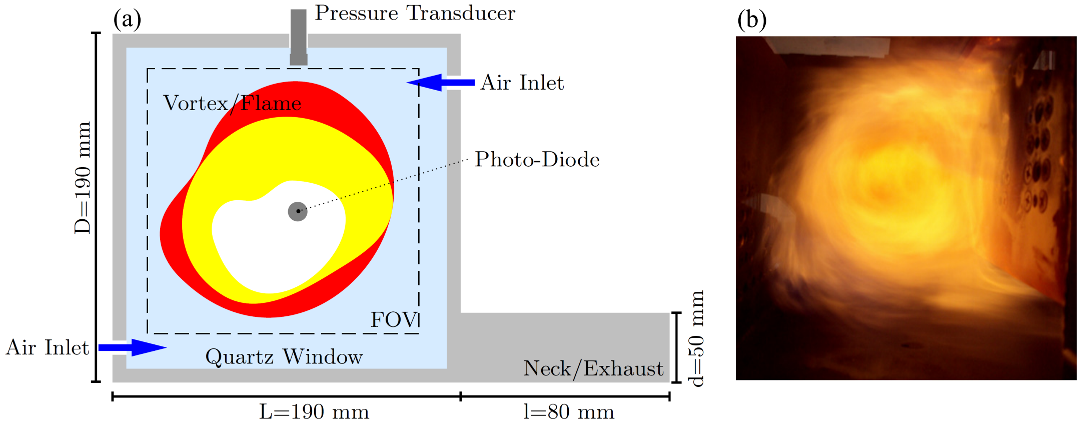

Figure 1. (a) Sketch of the TVC geometry and air injection scheme. For the sake of clarity, the wave guide employed for pressure measurement and methane inlets are not rendered. (b) Picture of the flame snapped through the side quartz window of the combustor.

3. Experimental set-up

TVC is realized as a cubic 190 mm cavity with an exhaust 80 mm in length, as sketched in figure 1a. Methane and air are separately injected through several inlets, distributed on the TVC side walls, and mixed by the large vortex generated into the TVC cavity. This can be visualized in figure 1b, displaying a picture of the flame taken through a large side quartz window, where the main reactive vortex can be clearly distinguished as filling up almost the whole cavity volume.

The inner pressure (p) is acquired by using a pressure transducer (Kulite XTEH-10L-190M), with a cut–off frequency equal to 20 kHz, connected to the cavity through a wave–guide. Instead, the radiant energy (E) emitted by the flame is sampled by a photo–diode (blue/UV enhanced silicon model 1053D with wavelength response from 300 to 1100 nm, as reported by [18]), placed in front of the quartz window. The photo–diode was not equipped with lenses to maximize its angle of view, embracing the whole combustion chamber volume. Both pressure and radiant energy time histories are synchronously acquired at 200 kHz for 30 s.

4. Results

TVC behaviour is tested at different power values and equivalence ratios. In order to give a preliminary characterization of each operating condition, the thermoacoustic efficiency is calculated as the ratio between acoustic power, P_a, and thermal power, P_t [26]:

$$\eta_{ta} = \frac{P_a}{P_t} = \frac{\langle p'^2 \rangle Z_0^{-1}}{\dot{m}_f \Delta H_f} \tag{8}$$

where Z_0 is the estimated characteristic acoustic impedance, $\dot{m}_f$ the measured fuel mass flow rate, and ΔH_f the propellant lower calorific value. A significant increase in η_{ta} (over an order of magnitude) is appreciated for $\phi = 0.6$ and $P_t = 69$ kW, which corresponds to gas flow rate of 7.9 $\mathrm{Nm^3/h}$ and total air flow rate of 191.2 $\mathrm{Nm^3/h}$, as shown in figure 2a.

All data analysis is focused on time series referred to this specific experimental condition because it leads the combustor to thermoacoustic instability, which often switches to abrupt extinction of the flame. Pressure (p) and radiant energy (E) signals are thus normalized to have zero mean and unitary standard deviation, and plotted in figure 2b and c, respectively. In particular, figure 2b displays a short time window of the pressure time series where, as expected, a regular and dominant periodic oscillation is appreciated; figure 2c reveals radiant

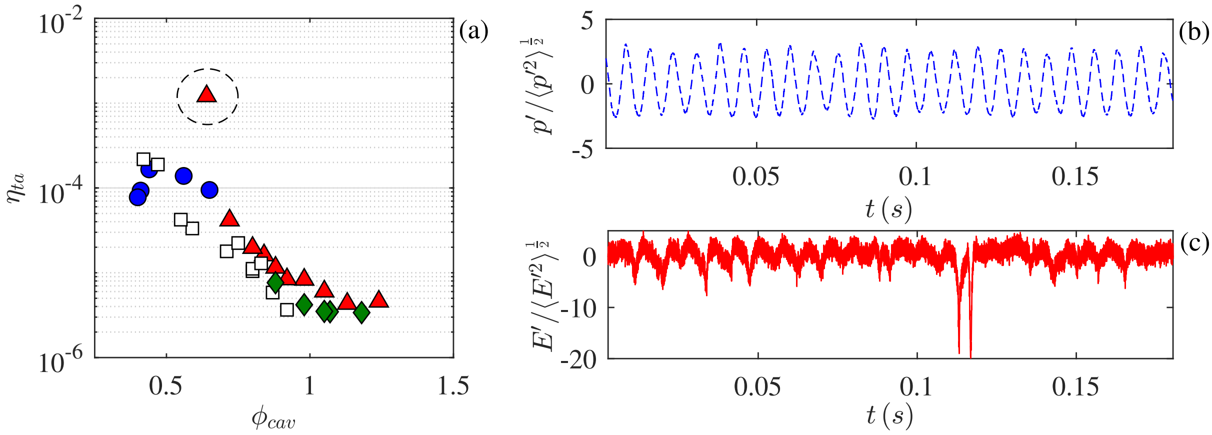

Figure 2. (a) Thermoacoustic efficiency upon the equivalence ratio computed for several operating conditions: $\circ$ refers to 53 kW, $\triangle$ to 69 kW, $\square$ to 70 kW, and $\diamond$ to 120 kW (black dashed circle marks the most efficient test case from thermo–acoustic view point); time histories of the normalized fluctuations of pressure (b) and radiant energy (c) for $\phi = 0.6$ and $P_t = 69$ kW.

energy exhibiting the same periodic oscillations as the pressure signal, superimposed to a broad–band component with random and rare sharp–negative–peaks. Signal post–processing (pre–qualification and wavelet analysis) is accomplished by an *ad hoc* software, as described in secs. 4.1 and 4.2.

4.1. Time series pre–qualification

The dominant periodic oscillation, revealed in pressure and radiant energy signals, is non–sinusoidal in both cases, as confirmed by their power spectral densities (PSDs) displayed in figure 3a, where the fundamental ($f_1 = 137$ Hz) and several harmonics (*e.g.* f_2 and f_3) emerge. In addition, in PSDs the harmonics of pressure and radiant energy are found at the same positions along frequency axis, confirming the important coupling between pressure and radiant energy fluctuations.

With the aim of gaining a statistical description of the two time series, probability density functions (PDFs) are superimposed to the normal distribution, as reported in figure 3b. Pressure PDF exhibits bi–modal shape, typical of limit cycle states. On the other hand, radiant energy signal displays heavy– and left long–tailed PDF, characteristic for events following an extreme value statistics [27]. The presence of the heavy long tail in radiant energy PDF is ascribable to negative peaks arising in the radiant energy time series (fig.2c). These peaks have been already observed by [12], who suggest their occurrence can be related to small–time–scale flame loss. However, to the best of our knowledge, a statistical analysis and characterization of such events is still lacking. Hence, focus of this work is an in-depth investigation of negative peaks, hereafter denoted as *drops*, pointed out in the radiant energy time series.

The phase portrait in figure 3d permits to further investigate the coupling between intermittent events in radiant energy and the pressure signal. Since both pressure and radiant energy are normalised with respect to their own standard deviation, a circular domain ($\mathcal{L}$) of radius equal to 3 is drawn for delimiting the phase–space region where these two observables occur with highest probability. Trajectories exceeding $\mathcal{L}$ boundaries are representative of intermittent phenomena in radiant energy. More specifically, during the drops in radiant energy signal, the trajectories are pushed outside $\mathcal{L}$ and then re-injected back into the inner region. Moreover, a statistical synchronization between the drops and pressure fluctuations can be observed: exceeding trajectories more often go through the third quadrant of the figure, where both

Journal of Physics: Conference Series **1589** (2020) 012005 doi:10.1088/1742-6596/1589/1/012005

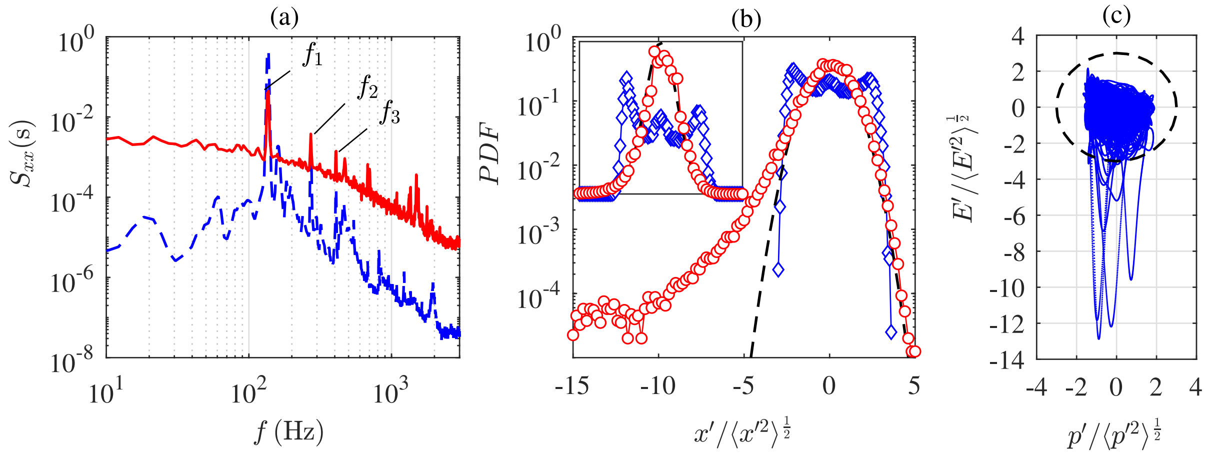

Figure 3. (a) Power spectral density of the normalised radiant energy (red solid-line) and pressure fluctuations (blue dashed-line);(b) probability density functions: $\circ$ refers to radiant energy, $\diamond$ marks pressure variable; (c) normalised pressure upon radiant energy phase portrait; dashed line is a circular domain of radius equal to 3.

pressure fluctuations and radiant energy assume negative values. This latter aspect is in full agreement with the experimental results provided by [12].

4.2. Wavelet analysis

The radiant energy signal is analysed by applying the wavelet–based auto–conditioning technique. The main steps of the procedure are listed in the following: *i)* as a first step, LIM, as defined in eq.5, is calculated over the entire signal. Since we are interested in intermittent events, it is worth looking in particular at drops occurring along the time history; *ii)* WBAT is applied to the radiant energy time series, succeeding in capturing instantaneous drops and computing the average signature of the signal. For the present analysis, the LIM threshold is fixed to 10, that is an order of magnitude over $LIM = 1$ [15], which marks the minimum value to overcome to address intermittency. This choice ensures only highly energetic events are detected, which are supposed to be the footprint of the flame blow-out [12].

An example of the outcome of this analysis is reported in fig.4a, where a single structure upon local time variable, ξ, emerges. This *average* signature, which resembles the *instantaneous* structures already identified by [12] in raw time series, appears as a negative–peak, of about 2 ms in time scale and over 3 times the signal standard deviation in amplitude.

Attempting to provide a more detailed description of the signature here identified, we proposed to interpret the descending branch as due to local extinction, while the ascending branch as representative of a sudden re–ignition induced by the accumulation of fresh mixture in combustion chamber. A fluctuating component is observed in the average signature plotted in figure 4a, despite drops occur randomly. In other words, this periodic component is not cancelled by the averaging process, implying a phase locking between it and random drops. As expected, this result, combined with phase–portrait reported in figure 3c, confirms that the probability of an extinction event increases when both pressure and radiant energy undergo a negative fluctuation. Moreover, the presence of an asymmetry in the drop is due to an overshooting located in the right branch of the drop and partially hidden by the periodic component. That overshooting is probably due to the accumulation of fresh mixture during the blowout phase.

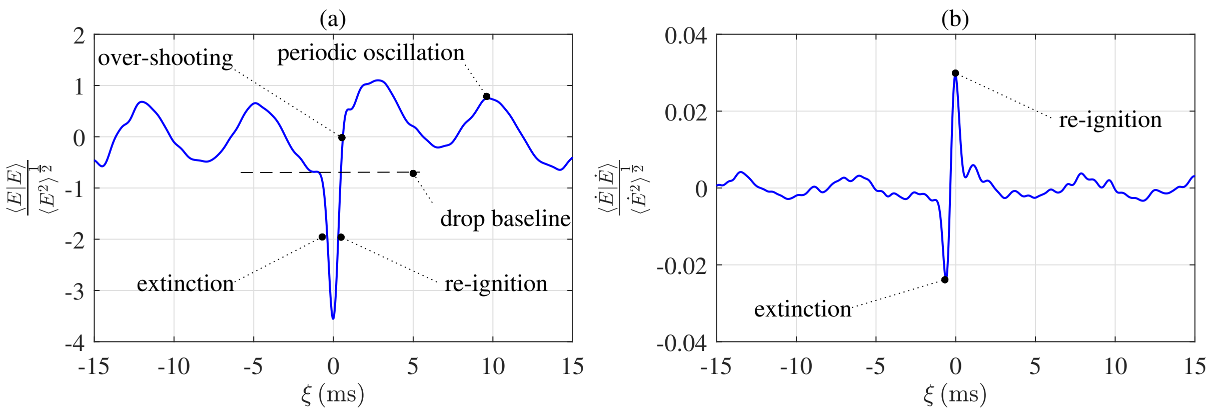

Figure 4. (a) Signatures calculated by applying the WBAT to the radiant energy (a) and to the radiant power (b) time histories.

In figures 4b the average signature calculated from the radiant power defined as follows:

$$\dot{E} = \frac{dE}{dt} \tag{9}$$

is a negative–positive peak structure. The negative part corresponds to the blowout phase while the positive peak can be referred to the re–ignition phase. Maximum and minimum values of the signature are quite different suggesting that the re–ignition is more abrupt than the extinction. This result is very interesting and highlights the potential of $\dot{E}$ for blowout diagnostics.

5. Conclusions

The thermoacoustic instability regime of a trapped vortex combustor is studied focusing on the radiant energy or power emitted by the flame. Wavelet transform of the raw signal provides the starting point for further analysis leading to an in–depth description of intermittent phenomena. WBAT is used to identify the average intermittent event, associated to the extinction–reignition of the combustor. A phase locking between random radiant energy drops and the signal periodic component is also observed. To the best our knowledge, this is the first time a wavelet–based autoconditioning technique is applied to combustion.
Wavelet transforms appear as powerful tools to tackle the study of thermoacoustic instability.

References

[1] L. Kabiraj and R. I. Sujith. Nonlinear self-excited thermoacoustic oscillations: intermittency and flame blowout. *J. Fluid Mech.*, 713:376–397, 2012.
[2] H. Gotoda, H. Nikimoto, T. Miyano, and S. Tachibana. Dynamic properties of combustion instability in a lean premixed gas-turbine combustor. *Chaos*, 21(1):013124, 2011.
[3] L. Kabiraj, A. Saurabh, P. Wahi, and R.I. Sujith. Route to chaos for combustion instability in ducted laminar premixed flames. *Chaos*, 22(2):023129, 2012.
[4] L. Kabiraj, R.I. Sujith, and P. Wahi. Investigating the dynamics of combustion-driven oscillations leading to lean blowout. *Fluid Dyn. Res.*, 44(3):031408, 2012.
[5] V. Nair, G. Thampi, and R.I. Sujith. Intermittency route to thermoacoustic instability in turbulent combustors. *J. Fluid Mech.*, 756:470–487, 2014.
[6] S. Chiocchini, T. Pagliaroli, R. Camussi, and E. Giacomazzi. Chaotic and linear statistics analysis in thermoacoustic instability detection. *J. Propul. Power*, 34(1):15–26, 2017.
[7] E. Giacomazzi, G. Troiani, E. Giulietti, and R. Bruschi. Effect of turbulence on flame radiative emission. *Exp. Fluids*, 44(4):557–564, 2008.

[8] T. Pagliaroli and R. Camussi. Acoustic and aeroacoustic characterization of rectangular partial enclosures. In *19th AIAA/CEAS Aeroacoustics Conference*, page 2050, 2013.

[9] T. Pagliaroli and R. Camussi. Wall pressure fluctuations in rectangular partial enclosures. *J. Sound Vib.*, 341:116–137, 2015.

[10] R. Hernandez, G. Troiani, T. Pagliaroli, and A. Hernandez-Guerrero. Chaotic analysis of the thermoacoustic instabilities of a trapped vortex combustor. In *2018 AIAA/CEAS Aeroacoustics Conference*, page 4104, 2018.

[11] R. Hernandez-Rivera, G. Troiani, T. Pagliaroli, and A. Hernandez-Guerrero. Detection of the thermoacoustic combustion instabilities of a slot burner based on a diagonal-wise recurrence quantification. *Physics of Fluids*, 31(12):124105, 2019.

[12] S. Nair and T. Lieuwen. Acoustic detection of blowout in premixed flames. *J. Prop. and Power*, 21(1):32–39, 2005.

[13] R. Camussi, G. Robert, and M. C. Jacob. Cross-wavelet analysis of wall pressure fluctuations beneath incompressible turbulent boundary layers. *J. of Fluid Mech.*, 617:11–30, 2008.

[14] R. Camussi and G. Guj. Orthonormal wavelet decomposition of turbulent flows: intermittency and coherent structures. *J. Fluid Mech.*, 348:177–199, 1997.

[15] M. Farge. Wavelet transforms and their applications to turbulence. *Annu. Rev. Fluid Mech.*, 24(1):395–458, 1992.

[16] C. Torrence and G. P. Compo. A practical guide to wavelet analysis. *Bull. Am. Meteorol. Soc.*, 79(1):61–78, 1998.

[17] E. Stefanutti and F. Bruni. Signal denoising using the stationary wavelet decomposition. In *IMEKO TC19 Workshop on Metrology for the Sea, MetroSea 2017: Learning to Measure Sea Health Parameters*, volume 2017-October, pages 104–110, 2017.

[18] T. Pagliaroli, R. Camussi, E. Giacomazzi, and E. Giulietti. Velocity measurement of particles ejected from a small-size solid rocket motor. *J. Prop. and Power*, 31(6):1777–1784, 2015.

[19] T. Pagliaroli, M. Mancinelli, G. Troiani, U. Iemma, and R. Camussi. Fourier and wavelet analyses of intermittent and resonant pressure components in a slot burner. *J. Sound Vib.*, 413:205–224, 2018.

[20] T. Pagliaroli, F. Patanè, A. Pagliaro, P. Lv, and A. Tatí. Metamaterials for hypersonic flow control: Experimental tests on novel ultrasonically absorptive coatings. In *2018 5th IEEE International Workshop on Metrology for AeroSpace (MetroAeroSpace)*, pages 284–289, June 2018.

[21] T. Pagliaroli, A. Pagliaro, F. Patanè, A. Tatì, and P. Lv. Wavelet analysis ultra-thin metasurface for hypersonic flow control. *Applied Acoustics*, 157:107032, 2020.

[22] J. Ashmead. Morlet wavelets in quantum mechanics. *Quanta*, 1(1):58–70, 2012.

[23] S. Mallat. *A wavelet tour of signal processing.* Academic press, 3rd edition, 2009.

[24] M. Mancinelli, T. Pagliaroli, A. Di Marco, R. Camussi, and T. Castelain. Wavelet decomposition of hydrodynamic and acoustic pressures in the near field of the jet. *J. Fluid Mech.*, 813:716–749, 2017.

[25] R. Camussi and G. Guj. Experimental analysis of intermittent coherent structures in the near field of a high re turbulent jet flow. *Phys. Fluids*, 11(2):423–431, 1999.

[26] W. C. Strahle. On combustion generated noise. *J. Fluid Mech.*, 49(02):399–414, 1971.

[27] E. Castillo, A. S. Hadi, N. Balakrishnan, and J. Sarabia. *Extreme value and related models with applications in engineering and science.* Wiley Hoboken, NJ, 2005.